Nutrigonometry I: Using Right-Angle Triangles to Quantify Nutritional Trade-Offs in Performance Landscapes

Juliano Morimoto,[1,2,3,*] Pedro Conceição,[3] Christen Mirth,[4] and Mathieu Lihoreau[5]

1. School of Biological Sciences, University of Aberdeen, Zoology Building, Tillydrone Avenue, Aberdeen AB24 2TZ, United Kingdom; 2. Programa de Pós-graduação em Ecologia e Conservação, Universidade Federal do Paraná, Curitiba 82590-300, Brazil; 3. Institute of Mathematics, University of Aberdeen, King's College, Aberdeen AB24 3FX, United Kingdom; 4. School of Biological Sciences, Monash University, Melbourne, Victoria, Australia; 5. Research Center on Animal Cognition (CRCA), Center for Integrative Biology (CBI), CNRS, University Paul Sabatier–Toulouse III, Toulouse, France

Submitted May 20, 2022; Accepted October 19, 2022; Electronically published March 22, 2023

Online enhancements: supplemental PDF.

ABSTRACT: Animals regulate their food intake to maximize the expression of fitness traits but are forced to trade off the optimal expression of some fitness traits because of differences in the nutrient requirements of each trait ("nutritional trade-offs"). Nutritional trade-offs have been experimentally uncovered using the geometric framework for nutrition (GF). However, current analytical methods to measure such responses rely on either visual inspection or complex models of vector calculations applied to multidimensional performance landscapes, making these approaches subjective or conceptually difficult, computationally expensive, and, in some cases, inaccurate. Here, we present a simple trigonometric model to measure nutritional trade-offs in multidimensional landscapes (nutrigonometry) that relies on the trigonometric relationships of right-angle triangles and thus is both conceptually and computationally easier to understand and use than previous quantitative approaches. We applied nutrigonometry to a landmark GF data set for comparison of several standard statistical models to assess model performance in finding regions in the performance landscapes. This revealed that polynomial (Bayesian) regressions can be used for precise and accurate predictions of peaks and valleys in performance landscapes, irrespective of the underlying structure of the data (i.e., individual food intakes vs. fixed diet ratios). We then identified the known nutritional trade-off between life span and reproductive rate in terms of both nutrient balance and concentration for validation of the model. This showed that nutrigonometry enables a fast, reliable, and reproducible quantification of nutritional trade-offs in multidimensional performance landscapes, thereby broadening the potential for future developments in comparative research on the evolution of animal nutrition.

Keywords: nutritional geometry, trigonometry, life span–reproduction trade-off, fitness maps.

* Corresponding author; email: juliano.morimoto@abdn.ac.uk.

ORCIDs: Morimoto, https://orcid.org/0000-0003-3561-1920; Conceição, https://orcid.org/0000-0003-3564-7587; Mirth, https://orcid.org/0000-0002-9765-4021; Lihoreau, https://orcid.org/0000-0002-2463-2040.

Introduction

Animals often require different nutrient blends to maximize concurrent life history traits, creating the potential for a conflict for optimum nutrition (Simpson and Raubenheimer 2012; Raubenheimer and Simpson 2020). When the optimum nutrition for two traits cannot be achieved simultaneously, animals must make a compromise in their feeding decisions to support the optimal expression of one trait over another ("nutritional trade-off"; Lee et al. 2008; Maklakov et al. 2008). Previous research has identified nutritional trade-offs between life span and reproduction or between immunity and reproduction across many different taxa, including *Drosophila melanogaster* (Ponton et al. 2019), tephritid fruit flies (Fanson and Taylor 2012; Fanson et al. 2012), crickets (Harrison et al. 2014; Treidel et al. 2021; Guo et al. 2022), and mice (Solon-Biet et al. 2014) (for reviews, see Ponton et al. 2011; Schwenke et al. 2016). Even traits related to different aspects of the same life history can vary in nutritional requirements during the lifetime of an animal, as seen, for instance, in pre- and postmating traits related to reproduction of many insect species, such as sperm number and viability (Bunning et al. 2015), fertilization success across sperm competitive contexts (Morimoto and Wigby 2016), cuticular hydrocarbons, and courtship song and sperm viability (Ng et al. 2018) as well as size and numbers of eupyrene and apyrene sperms (Gage and Cook 1994). Thus, nutritional trade-offs are likely ubiquitous and impose significant constraints on the feeding choices of individuals.

Measuring nutritional trade-offs is critical to understanding the evolution of animal feeding behavior. However, it is highly challenging because of the interactive

effects of nutrient ratios and concentrations on the expression of life histories (Stearns 1992; Roff 2002; Hunt et al. 2004; Simpson and Raubenheimer 2012). In recent decades, however, a method known as the geometric framework for nutrition (GF) has emerged as a powerful unifying framework capable of disentangling the multidimensional effects of nutrients (both ratios and concentrations) on life history traits and fitness (Raubenheimer and Simpson 1993). The GF has been applied to a diverse range of nutritional studies across species such as flies (Lee et al. 2008; Fanson and Taylor 2012; Jensen et al. 2015; Ponton et al. 2015; Barragan-Fonseca et al. 2018), crickets (Maklakov et al. 2008; Ng et al. 2018; Rapkin et al. 2018), cockroaches (Bunning et al. 2015), domestic cats and dogs (Hewson-Hughes et al. 2011, 2013), and mice (Solon-Biet et al. 2014; Morimoto et al. 2019), being paramount for advancing our understanding of complex physiological and behavioral processes across ecological environments and even human health (Simpson et al. 2017). With the growing applications of GF in the study of animal and human nutrition, the development of simple, intuitive, and accurate quantitative methods for identifying optimal diets in performance landscapes and quantifying nutritional trade-offs has become a key issue for research in comparative nutrition. Simple methodologies that are friendly to biologists and ecologists will facilitate new insights into the complex nutritional decision-making that animals have to undergo in order to navigate physiological and behavioral constraints of different life history traits (Morimoto and Lihoreau 2020).

Recent approaches to analyze GF data have been complex to navigate, and many studies continue to use a combination of approaches (including visual inspection) or potentially inaccurate methods to quantify the strength of nutritional trade-offs in GF landscapes (Polak et al. 2017; Ng et al. 2018, 2019; Rapkin et al. 2018; Kutz et al. 2019; Morimoto and Lihoreau 2019; Ma et al. 2020; Barragan-Fonseca et al. 2021). There are three major gaps in our approaches to analyzing GF data that contribute to inconsistencies in the analysis in the field of nutritional ecology: (i) there has been no investigation into the suitability and accuracy of different statistical models in identifying regions of interest (e.g., peaks, valleys) in multidimensional performance landscapes (see, e.g., Rapkin et al. 2018; Morimoto and Lihoreau 2019). The reason for this is because (ii) current methods to analyze multidimensional GF performance landscapes are complex and difficult to implement in a comparative fashion, precluding the exploration of the full range of statistical methods commonly used in ecology and evolution (e.g., linear regressions, additive models). Moreover, (iii) the structure of the data that GF empirical studies generate is also inconsistent. For instance, some GF studies measure both the amount of food ingested and the trait values on each diet across a broad range of dietary compositions (e.g., Maklakov et al. 2008), while others consider diets as treatments and examine the effect of a wide range of diets on trait values without measuring food intake (e.g., Kutz et al. 2019). This difference in experimental approach leads to distortions in the generated performance landscapes that could influence the estimates of the strength of nutritional trade-offs. No study has investigated how current analytical methods perform in identifying peaks and valleys across different data structures. Collectively, these gaps in analytical methods used to estimate nutritional trade-offs limit our ability to draw conclusions between studies and, more broadly, preclude our understanding of the evolution of nutritional responses in comparative analysis. Thus, there is a need for the development of consistent analyses that derive precise estimates of peak (and valley) regions from GF landscapes, thereby enabling large-scale comparative analyses necessary to gain insights into the evolution of animal nutrition.

Here, we address these gaps by proposing a novel analytical model (nutrigonometry) that is simple and precise and that can accommodate different data structures. We then use this model to conduct the first comparative analysis of different statistical methods and their performance in identifying regions of interest (e.g., peaks or valleys) in GF performance landscapes. Nutrigonometry is different from our previous vector of positions approach (Morimoto and Lihoreau 2019) because the latter used a single statistical model (i.e., a support-vector machine [SVM] model) that required an arbitrary input threshold to identify peak regions. Moreover, the vector of positions could not identify and delineate valley regions as accurately and the overall approach was computationally expensive to apply to multiple landscapes. Nutrigonometry uses trigonometric relationships (i.e., the Pythagorean theorem) to estimate the difference in angles of right-angle triangles formed in performance traits (fig. 1*a*), after which the difference between these angles can be estimated as a proxy for the strength of nutritional trade-offs (i.e., wider angles indicate stronger trade-offs; fig. 1*b*).

Below, we first describe the mathematical foundation underlying the nutrigonometry method. Next, we apply nutrigonometry to a landmark GF data set in *D. melanogaster* with known nutritional trade-offs between life span and reproductive rate (Lee et al. 2008; Morimoto and Lihoreau 2019). This data set provided an important ground truth to apply, test, and validate the precision of nutrigonometry in identifying the known nutritional trade-off. Moreover, the use of this data set allowed us to demonstrate the consistency of the nutrigonometry model in identifying nutritional trade-offs when the structure of the input data set varied (i.e., individual intake vs. fixed

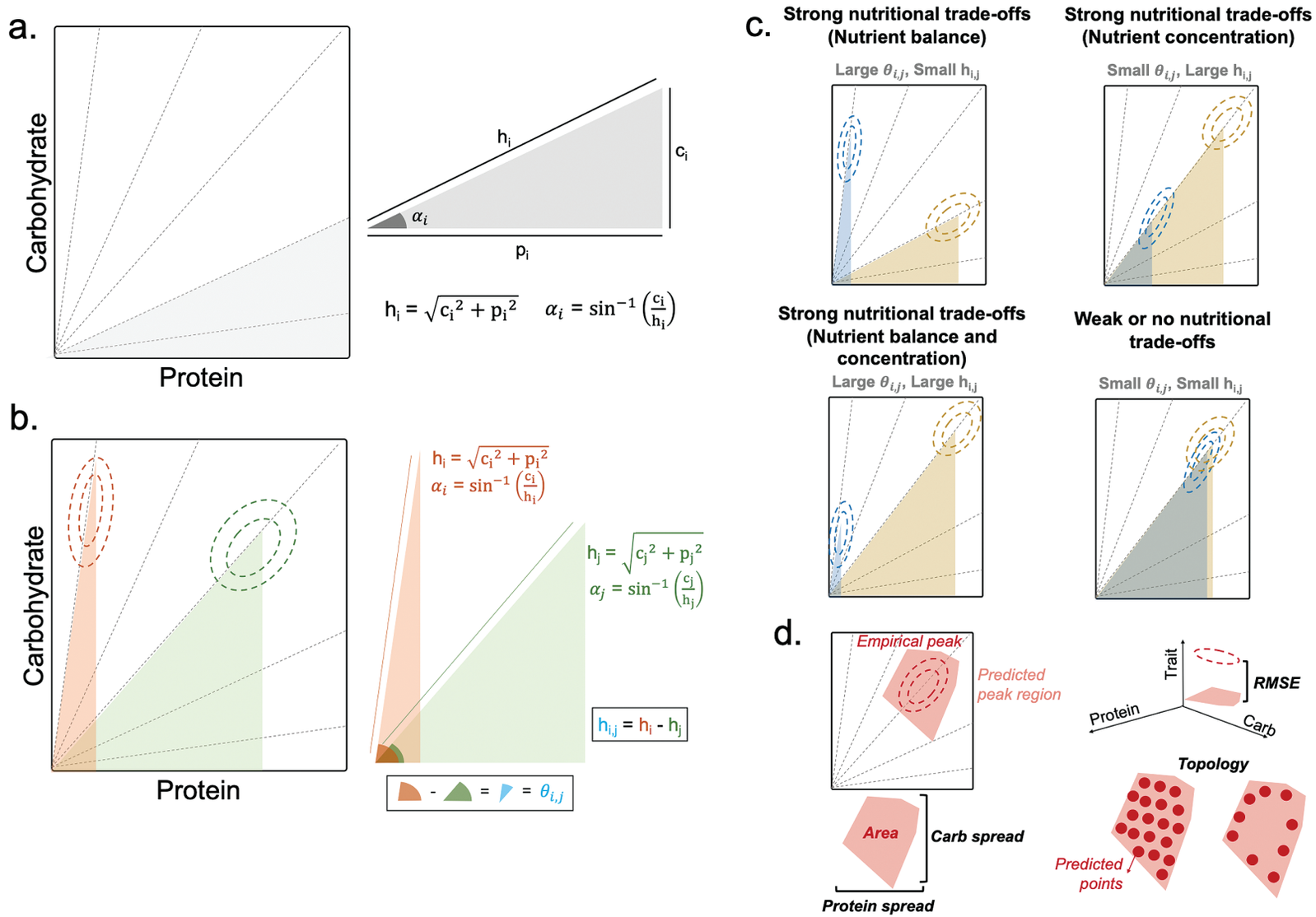

Figure 1: Nutrigonometry model. *a*, Considering an infinite number of nutritional rails that divide the nutritional space into right-angle triangles, the angle α_i and the hypotenuse h_i can be calculated from trigonometric relationships. *b*, Nutrigonometry allows for the estimates of the strength of nutritional trade-offs in terms of nutrient balance (angle $\theta_{i,j}$) and nutrient concentration (the difference $h_{i,j}$, given in absolute terms). *c*, Scenarios for the estimates of the strength of nutritional trade-offs with respect to the angle $\theta_{i,j}$ and the length $h_{i,j}$. *d*, Metrics used for the peak prediction in the 3D landscape (for details, see "Methods"). RMSE = root mean square error.

ratio experiments). Finally, we leveraged the simplicity (and computationally cheap) approach provided by nutrigonometry to conduct the first comparative analyses of a range of "off-the-shelf" statistical models (including machine learning) in estimating the peak region in the performance landscapes, which is an essential component for proper quantification of nutritional trade-offs.

Material and Methods

Nutrigonometry

GF studies consider a "nutritional space" in which animals can eat foods and navigate their nutritional state (for a review, see Raubenheimer and Simpson 2020). This nutritional space is defined by the food components (typically macronutrients) under investigation. Foods are represented in the nutritional space as nutritional rails (i.e., imaginary lines that pass through the origin with a given positive slope) characterized by different ratios of the food components. For example, in studies where protein and carbohydrate effects are investigated, there is a 2D nutritional space (one dimension for each nutrient) onto which the performance landscape of the trait is mapped. This rationale can be extended to n number of nutrients (Simpson and Raubenheimer 1993), although to date studies with two nutrients are the most common (Morimoto and Lihoreau 2020). If we consider this 2D nutritional space as a rectangular space in which an infinite number of nutritional rails (i.e., foods) exist that divides the space in right-angle triangles, then it is possible to use simple trigonometric functions to estimate the angle α_i and the hypotenuse of the triangle for all fitness traits mapped onto the nutritional space. The angle α_i is the angle of the nutritional rail, relative from the x-axis, that passes through the peak in the landscape for the trait i, and the hypotenuse h_i of the triangle shows how far from the origin the peak in the landscape sits for trait i (fig. 1*a*). Both α_i and h_i can be calculated using the Pythagorean theorem and the relationship between the angle and the sides of right-angle triangles (i.e., sines and cosines), as shown in figure 1*a*.

Once α_i and α_j are known, we can estimate the angle θ (as in Morimoto and Lihoreau 2019), which is the difference in the angle between nutritional rails that maximize two traits, i and j, and provides a measure of the strength of the nutritional trade-off that exists between traits i and j (fig. 1*b*). The larger the angle $\theta_{i,j}$, the stronger the nutritional trade-off in terms of nutrient balance (and potentially nutritional compromise) between traits. Likewise, we can compare the difference $h_{i,j}$ in the estimates of the hypotenuse h_j and h_i^* to quantify nutritional trade-offs in relation to nutrient concentration (fig. 1*b*). These metrics allowed us to disentangle the following theoretical scenarios in which nutritional trade-off can occur (fig. 1*c*): (i) when $\theta_{i,j}$ is large but $h_{i,j}$ is small (strong nutritional trade-off in terms of nutrient balance); (ii) when $\theta_{i,j}$ is small but $h_{i,j}$ is large (strong nutritional trade-off in terms of nutrient concentration); (iii) when $\theta_{i,j}$ and $h_{i,j}$ are large (strong nutritional trade-off in terms of both nutrient balance and concentration); and (iv) when $\theta_{i,j}$ and $h_{i,j}$ are small (weak or no nutritional trade-off).

Here, when applying this model to empirical data sets (see below), inferences on the strength of nutritional trade-offs were made using confidence intervals for $h_{i,j}$ and $\theta_{i,j}$, whereby nutritional trade-offs were stronger when confidence intervals did not overlap zero and the magnitude of the difference was large. Estimates are presented in the units of the nutrient space in which the data were collected (e.g., mg), while angles are presented in degrees. Confidence intervals for both $h_{i,j}$ and $\theta_{i,j}$ were calculated using the significance threshold of .05 and the quartiles of a t distribution. All analyses and plots were done in R version 3.6.2 (R Core Team 2019).

Data Sets Used for Model Application: Diet Intake and Fixed Ratios

Nutrigonometry was designed to work on diverse types of GF data, including those generated from experimental approaches measuring diet intakes or fixed ratio diets (see the introduction). To validate this, we applied the nutrigonometry model to a landmark data set that measured the nutritional requirements for life span and reproduction in *Drosophila melanogaster* (Lee et al. 2008). This data set was used to test previous approaches and therefore has important benchmark status in the field, providing the ground-truth data for the identification of the now-known nutritional trade-offs between life span and reproductive rate (Morimoto and Lihoreau 2019). These data have the benefit of allowing us to implement the nutrigonometry model to measure the trade-off in data of both intake and fixed ratio structures. This is because the original data carefully estimated individual intake across diets and provided the ratio of nutrients of all diets, enabling us to transform the data structure from intake to fixed ratio. We also demonstrated the application of nutrigonometry to a GF data set with fixed ratios from Kutz et al. (2019), who studied how temperature modulates nutritional responses of larval development and adult fitness in *D. melanogaster*, as an auxiliary demonstration of the application of our model (see fig. S1).

Analytical Approach

The implementation outline of nutrigonometry is as follows.

Predicting peak (or valley) location and size. We designed algorithms that fitted a range of statistical models

(details of the models are given below) to the empirical data in order to test their performance in predicting peaks (or valleys; see the supplemental PDF) in the performance landscape for life span and reproductive rate from our landmark data set. This comparative statistical approach enabled us to provide the first comparative assessment of models to identify peak regions in GF performance landscapes. This was done for both the data set with nutrient intake and with fixed ratios. This enabled us to predict peak regions in the performance landscapes for which further analysis was possible.

Model fit. We then tested the fit of all models using several quantitative parameters, such as (i) root mean square error (RMSE), (ii) peak area and spread, and (iii) homogeneity of points within the predicted peak region. These provide information on the error in the predictive estimates of the performance trait in the *z*-axis, the spread that the models predicted the peak in the landscape to comprise, and the clustering of points that delineate the predicted peak region, respectively.

Nutrient balance. We then compared the nutrient ratio of the predicted peak regions with the nutrient ratio that animals chose when given the freedom to self-balance their diet (also known as the nutrient intake target). This allows the model to infer whether animals are maximizing any particular performance trait (i.e., the ratio of intake target coincides with the ratio of predicted peak). Below, we provide the details of each of the steps outlined above.

Predicting peak (or valley) location and size. As with previous approaches, our model depends on accurate estimates of the coordinates for the peak in the multidimensional performance landscape. Without this, estimates of $h_{i,j}$ and θ are inaccurate, which in turn affects the ability of the model to estimate the strength of nutritional trade-offs. To overcome this, the basic algorithms underpinning the identification of peak regions in performance landscapes were designed as follows: (*a*) empirical data were split into training (75%) and test (25%) data sets; (*b*) the statistical model was fitted to the training set using 10-fold cross validation, with the fitness trait as the dependent variable and the nutrient intakes (or fixed ratios) as the independent variables (the model included the main and interactive effects of protein and carbohydrate as well as the quadratic effects of each nutrient for nonlinear relationships); (*c*) a set of 500 random points corresponding to (protein, carbohydrate) coordinates were generated, and the model of step *b* was used to predict the value of the performance trait at these points and select the points with the highest 5% predicted performance trait values; and (*d*) step *c* was repeated 100 times.

Peak area was then estimated as the area of the convex hull incorporating all of the predicted points from the above-described algorithm. The ci function of the Rmisc package (Hope 2013) was used to estimate 95% confidence intervals of peak area.

We compared the performance of several statistical models (including commonly used statistical GF literature), namely, Bayesian linear regression (Bayes), general linear regression (LM), *k*-nearest neighbors (KNN), gradient boost (GBoost), random forest (RF), SVM with radial basis function, and generalized additive models (GAMs) with smooth term or tensor product terms. Note that SVM models were used as the underlying model in the vector of positions approach in Morimoto and Lihoreau (2020) and thus provides the grounds where the two methodologies can be compared. With the exception of GAMs that were fitted using the mgcv package (Wood and Wood 2015), all other models were fitted using the tidymodels package of the tidyverse (Wickham et al. 2019). Performance landscapes were estimated using the Tps function of the fields package (Nychka et al. 2017). We fitted the majority of models with default parameters, as these are the most likely approach from a beginner starting to work with GF data. Automated parameter tuning built into the tidymodels package was done for the mtry argument (RF and GBoost), the cost argument (SVM), and the neighbors and weight_func (KNN). For Bayes, we fitted a weakly informative Cauchy prior using the rstan::cauchy(. . .) function (Goodrich et al. 2020). All plots were constructed using the ggplot2 package (Wickham 2016). We also demonstrated how the best-performing models in our peak analyses can be used to predict valley regions in GF data sets (figs. S2, S3). The R code with the functions used for this article is available in the Dryad Digital Repository and Zenodo (Morimoto et al. 2022; https://doi.org/10.5061/dryad.5mkkwh78q).

Model Fit

RMSE. The RMSE was estimated as the difference between the predicted (generated by the above-described algorithm) and observed (from the empirical data set) values for the performance trait. Note that RMSE values do not interfere with the accuracy of estimates of $h_{i,j}$, and θ—and thus the estimates of nutritional trade-offs—because the *z*-axis is not used in the calculation of angles and hypotenuses (fig. 1*d*). A model can have a high RMSE and still be the best predictive model as long as the predicted peak correctly matches with the observed peak in the landscape.

Peak area. In addition to the RMSE, we estimated the area (in squared units in which the data are collected) of the polygon delimited by the estimated predicted peak region (area) and the horizontal (protein) and vertical (carbohydrate) spread of the data points of the predicted peak region (nutrient spread) as proxies for the precision

of our predicted peak regions (fig. 1*d*). The smaller the area and nutrient spread, the more compact the prediction of the peak region in the nutritional space.

Homogeneity of points within the predicted peak region. Even in cases where the RMSE, area, and nutrient spread of the predicted peak regions are small, it is important to have evenly spaced data points within the predicted peak region. This is because predictions of regions that contain holes can lead to misestimation of the strength of nutritional trade-offs by potentially adding noise to the set of protein and carbohydrate coordinates used to calculate $h_{i,j}$ and the angle θ. We measured the topological structure of the predicted peak region using the concept of persistence homology (PH), which in simple terms allows us to investigate the overall structural organization of the data (for details of the concept, see text S1; Zomorodian and Carlsson 2005; Weinberger 2011; fig. 1*d*). PH was estimated using the TDAstats package (Wadhwa et al. 2018). Together, the estimates of the RMSE, area, nutrient spread, and PH provided a comprehensive suite of metrics to assess the quality of model predictions for the peak region in fitness landscapes.

Nutrient Balance

Drosophila melanogaster adults balance their nutrient intake to a protein-to-carbohydrate (P : C) ratio of 1 : 4 when given the possibility to self-select multiple nutritionally complementary foods (see results in the original study, Lee et al. 2008). We then used the peak predictions of the nutrigonometry framework to test whether the observed P : C ratios that maximized life span and reproductive rates coincided with the P : C ratio of 1 : 4 reached by flies in choice situations. To achieve this, we calculated the 95% confidence interval as described for the peak area but in this case for the P : C ratio of each trait. Whenever the confidence interval overlapped 1 : 4, we inferred that the estimate of peak ratio did not statistically differ from the intake target of 1 : 4.

Results

Simple (Bayesian) Linear Regressions Outshine Machine Learning Models When Predicting Peak Region in Multidimensional Landscapes

First, we applied the nutrigonometry model with several underlying statistical models to test the precision of the framework in finding peak regions in the performance landscapes. All models generated predictions of peak region in nutritional landscapes irrespective of data structure, although the accuracy and topology of the predicted regions varied (figs. 2–4). In general, GAMs with tensor product and smooth function as well as Bayes and LM linear models generated peak predictions for both life span and reproductive rate that were significantly more precise (narrower) than other models when the structure of the data was composed of food intakes (fig. 2; tables S1, S2).

When the data structure changed to fixed ratios, LM, GAM with tensor product, Bayes, and KNN predicted peaks with smaller area for life span, and all but KNN perform within similar scales for the peak prediction of reproductive rate (fig. 3; tables S1, S2). In comparison, GAM smooth did not perform well in predicting a peak region that was homogenous and precise in the performance landscapes.

The performance of the models was independent of the estimates of the RMSE and nutrient spread, which showed no clear pattern of performance. The exceptions were that LM and Bayes displayed consistently lower spread when the structure of the data were intakes (figs. 4, 5; table S2).

Interestingly, machine learning models consistently underperformed, predicting peak regions that were wider and less precise (figs. 2–4; tables S1, S2). The underlying reason for this is unclear, but similar patterns were observed when predicting the peak region of the Kutz et al. (2019) data set (see fig. S1; table S3). This is important because the previous vector of position approaches uses SVM models, which, as shown here, do not perform as well as other simpler models (Morimoto and Lihoreau 2020). Bayes, GAMs (both smooth and tensor product), and LM also performed well when predicting valley regions (see figs. S2, S3). These results indicate that simple (Bayesian) linear regression consistently provides precise estimates of peak regions in performance landscapes irrespective of the structure of the data and that GAMs with tensor product (and to a smaller extent, smooth function) can also be used when the data structure is of individual intakes.

Precision in Estimates of Known Nutritional Trade-Offs in Performance Landscapes

Next, we tested whether nutrigonometry was capable of reliably quantifying known nutritional trade-offs in the data set. The data set used here contains a strong trade-off between life span and reproductive rate (Lee et al. 2008; Morimoto and Lihoreau 2019). We therefore tested how different statistical models in nutrigonometry performed when estimating this nutritional trade-off. GAMs (both smooth and tensor product), Bayes, LM, and KNN were the only models that correctly identified the known nutritional trade-off in the data set, measured by angle θ between life span and reproductive rate for data with individual intakes (table 1). Given the variability in the area, spread, and topology of the predicted region, estimates of

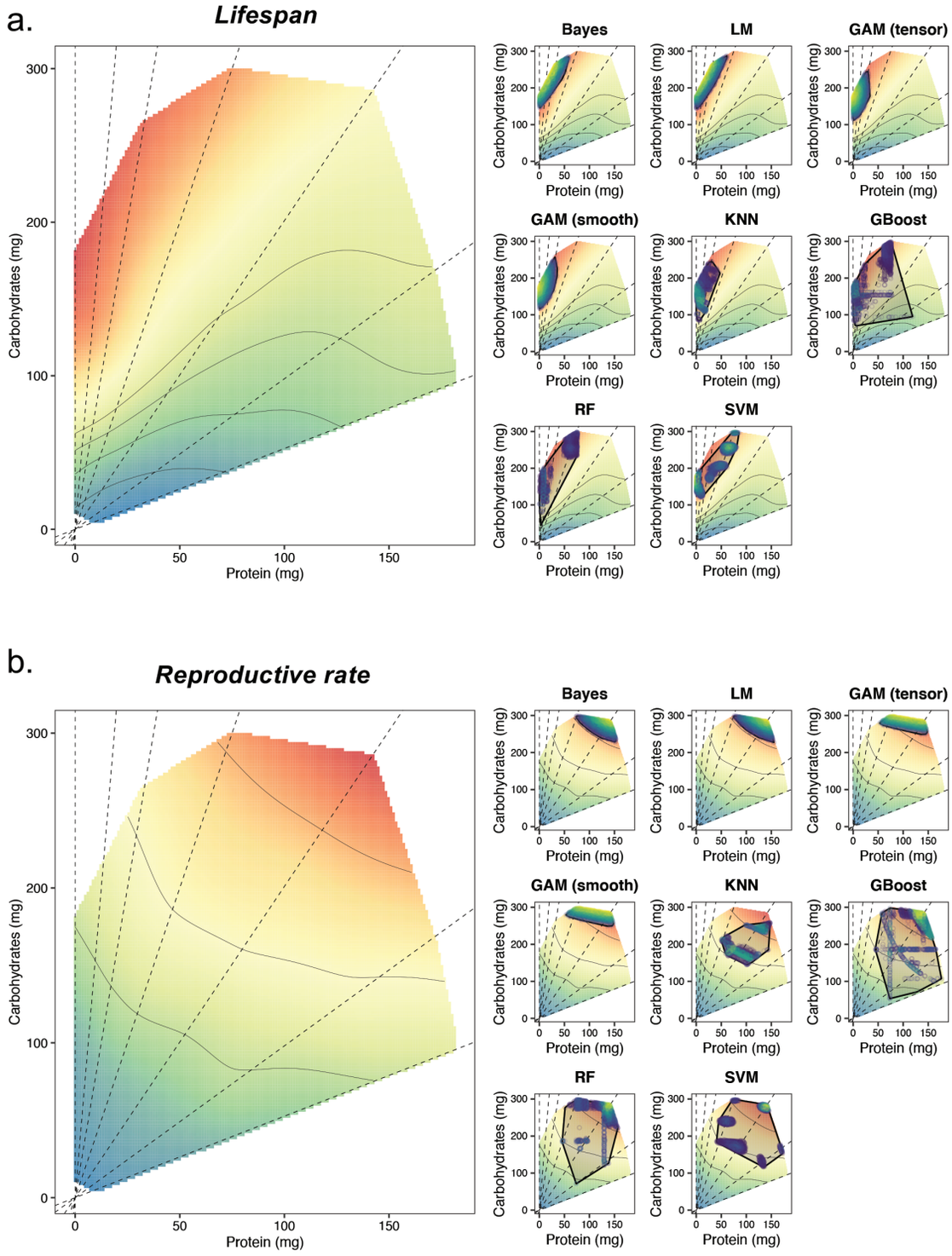

Figure 2: Predictions of peak region in life span and reproductive rate landscape with intake data. *a*, Life span landscape with the overlaid predicted peak regions (right small panels). *b*, Reproductive rate landscape with the overlaid predicted peak regions. Red represents peaks, while light green represents valleys. For the predicted region, dark blue represents points with lower predicted *z* values, whereas bright yellow represents points with higher predicted *z* values. Shaded polygon added to help visualization. Dashed lines represent the nutritional rails (i.e., foods with fixed P : C ratios) on which animals were allowed to eat. Bayes = Bayesian linear regression; GAM = generalized additive model; GBoost = gradient boost; KNN = *k*-nearest neighbors; LM = general linear regression; RF = random forest; SVM = support-vector machine.

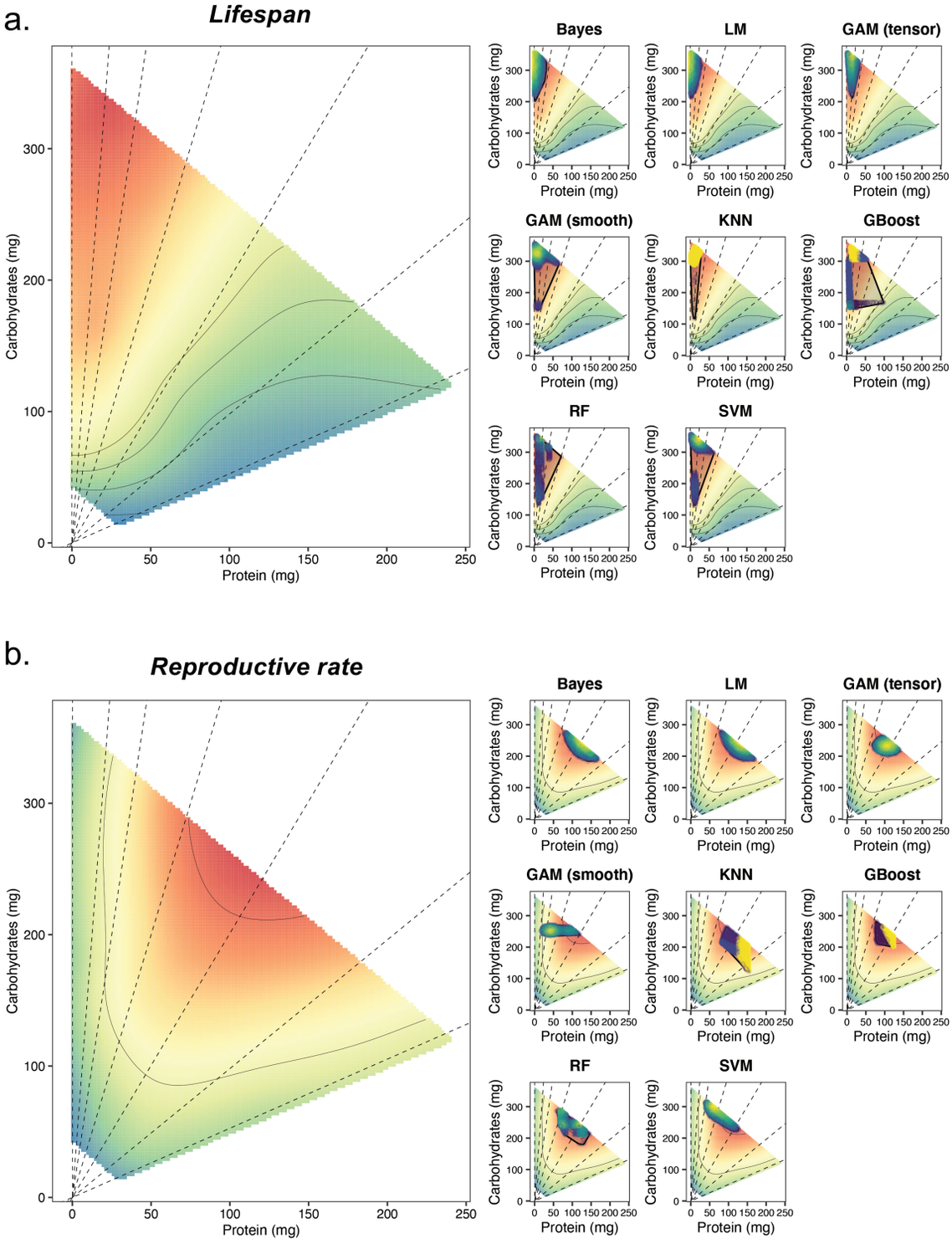

Figure 3: Predictions of peak region in life span and reproductive rate landscape with fixed ratio data. *a*, Life span landscape with the overlaid predicted peak regions (right small panels). *b*, Reproductive rate landscapes with the overlaid predicted peak regions. For the landscapes, red represents peaks, while light green represents valleys. For the predicted region, dark blue represents points with lower predicted *z* values, whereas bright yellow represents points with higher predicted *z* values. The shaded polygon was added to facilitate visualization of the predicted peak region and the homogeneity of points within the predicted peak. Bayes = Bayesian linear regression; GAM = generalized additive model; GBoost = gradient boost; KNN = *k*-nearest neighbors; LM = general linear regression; RF = random forest; SVM = support-vector machine.

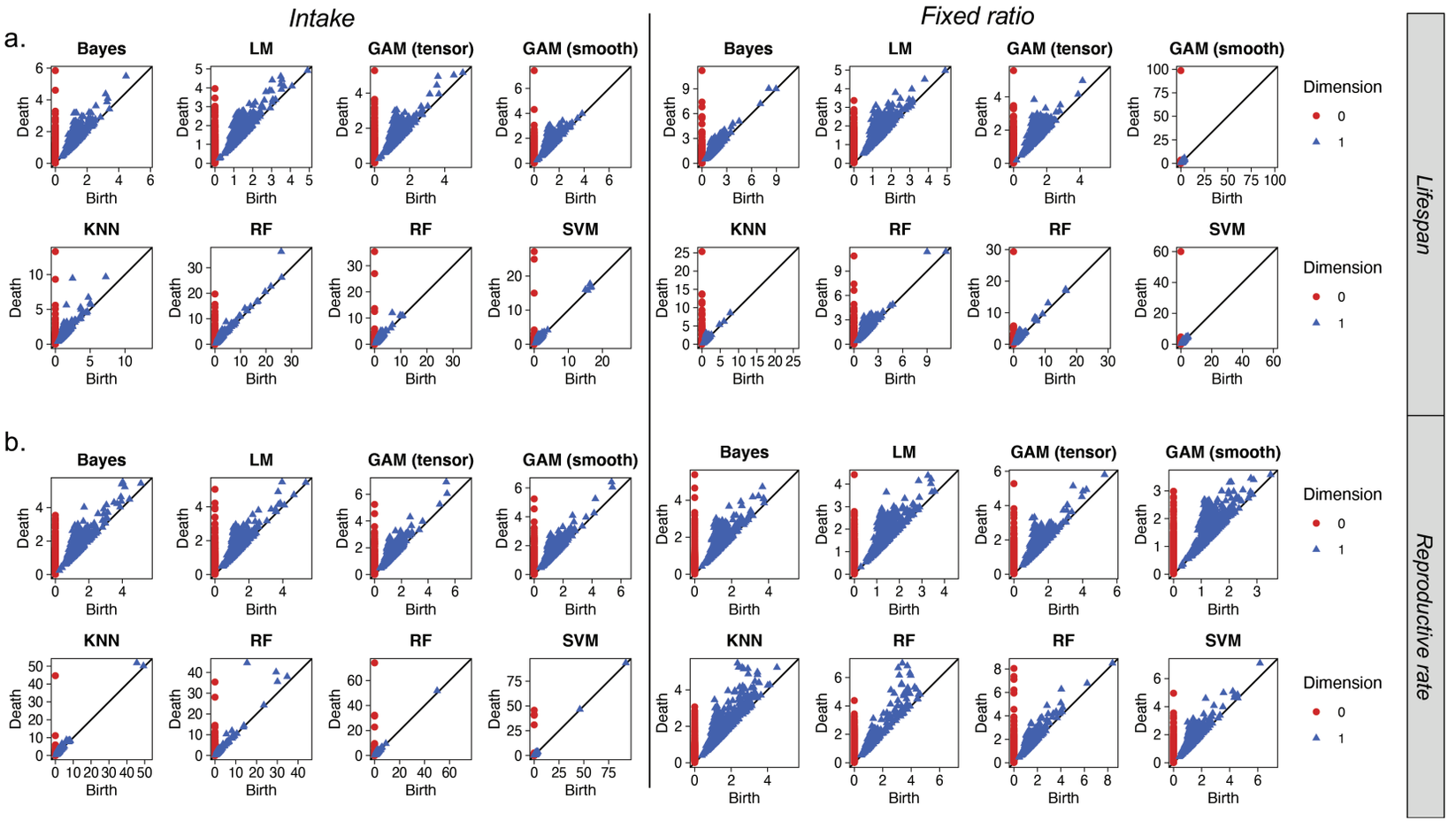

Figure 4: Persistence homology (PH) for the topological structure of the predicted peak region. *a*, PH plots of the predicted peak region in life span of data containing the structure of individual intake (*top left*) and fixed intake data (*top right*). *b*, PH plots of the predicted peak region in reproductive rate with data of structure containing individual intake (*bottom left*) and fixed intake data (*bottom right*). Homogenous predicted peaks have red (dimension 0) and blue (dimension 1) points that are closer, as opposed to more heterogeneous predicted peaks on which (some) points can be farther from each other. Bayes = Bayesian linear regression; GAM = generalized additive model; GBoost = gradient boost; KNN = *k*-nearest neighbors; LM = general linear regression; RF = random forest; SVM = support-vector machine.

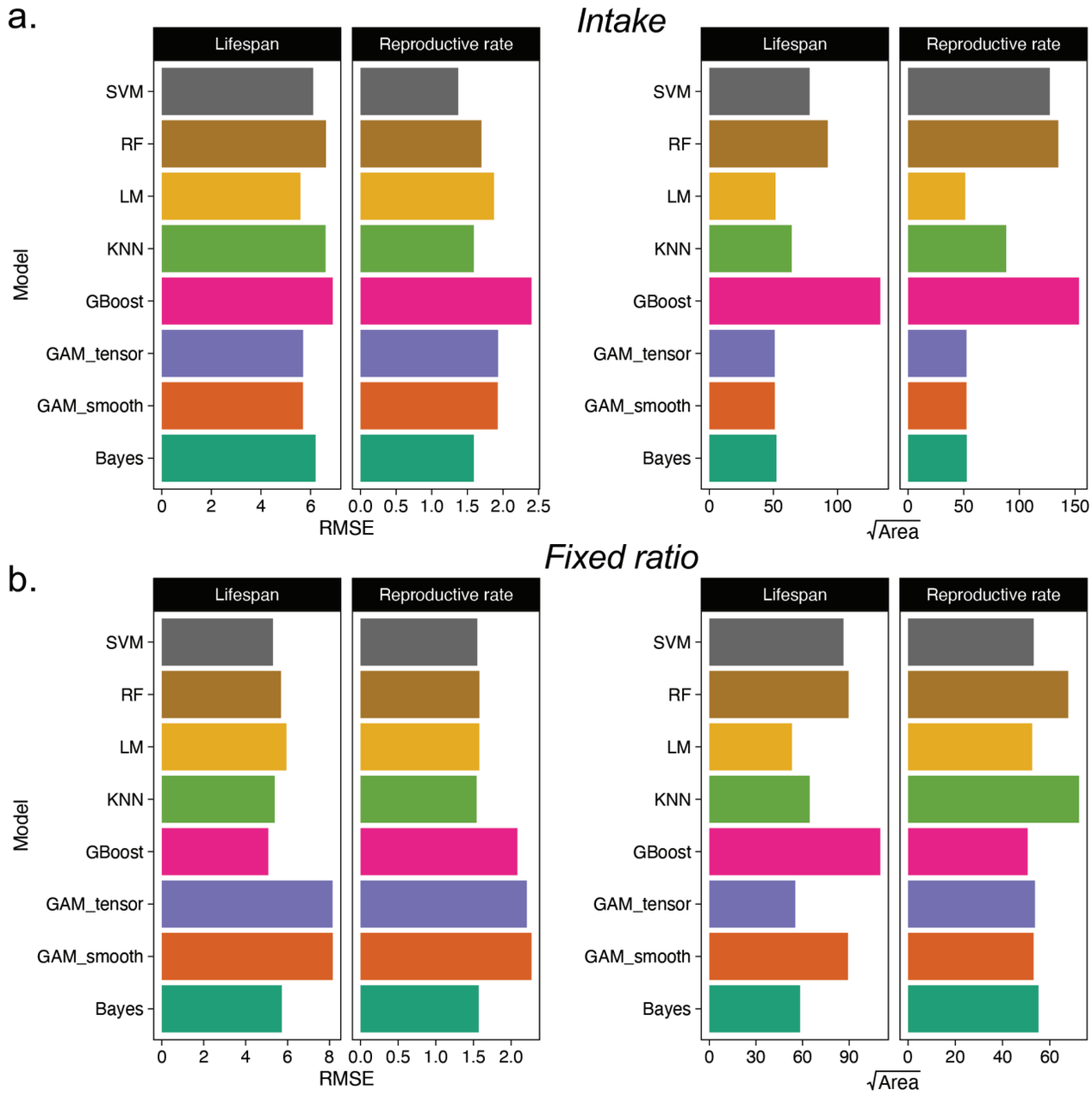

Figure 5: Root mean square error (RMSE) and peak area estimates in peak region predictions. *a*, RMSE and predicted peak area (i.e., area of the shaded polygon from the predicted region for life span and reproductive rate data), with structure containing individual intakes. *b*, RMSE and predicted peak area (i.e., area of the shaded polygon from the predicted region for life span and reproductive rate data), with structure containing fixed ratios. Note that models with a high RMSE can still be the best predictors of peak region. Bayes = Bayesian linear regression; GAM = generalized additive model; GBoost = gradient boost; KNN = *k*-nearest neighbors; LM = general linear regression; RF = random forest; SVM = support-vector machine.

$h_{i,j}$ and θ were more precise (narrower confidence intervals) for GAMs (smooth and tenor product), Bayes, and LM compared with KNN. GAMs, Bayes, and LM were the only models that identified a trade-off on the hypotenuse estimate $h_{i,j}$ for data of individual intakes, while KNN was the only model that identified this trade-off in data with fixed ratios (table 1). Thus, simpler models are overall more suitable to generating peak predictions that accurately

Table 1: Quantification of nutritional trade-offs between life span and reproduction

			Confidence interval	
Data, parameter, model	Estimate	SD	Lower	Upper
Trade-off (intakes):				
$\theta_{i,j}$:				
SVM	14.456	10.728	−6.574	35.485
RF	14.508	8.109	−1.388	30.404
GAM tensor	16.128	4.984	6.358	25.897
GAM smooth	16.166	4.962	6.438	25.893
GBoost	17.063	9.575	−1.706	35.831
LM	17.940	4.826	8.479	27.400
Bayes	18.205	4.709	8.974	27.436
KNN	21.203	6.181	9.088	33.318
$h_{i,j}$:				
SVM	16.792	65.723	−112.038	145.622
KNN	50.015	48.137	−44.343	144.373
GBoost	52.851	75.218	−94.591	200.293
RF	58.561	66.066	−70.943	188.064
LM	75.870	35.142	6.984	144.757
Bayes	76.729	34.444	9.211	144.247
GAM smooth	120.245	29.406	62.604	177.886
GAM tensor	124.533	27.930	69.784	179.282
Trade-off (fixed):				
$\theta_{i,j}$:				
GAM smooth	9.645	5.897	−1.916	21.205
SVM	11.840	5.649	.767	22.913
RF	17.368	5.848	5.906	28.831
GBoost	20.177	5.057	10.264	30.090
GAM tensor	21.177	3.872	13.588	28.766
Bayes	26.454	5.876	14.935	37.973
LM	26.499	5.903	14.928	38.070
KNN	31.428	7.186	17.342	45.513
$h_{i,j}$:				
SVM	2.381	68.888	−132.653	137.416
RF	4.819	64.841	−122.283	131.921
GBoost	9.377	65.605	−119.222	137.975
Bayes	41.461	34.912	−26.974	109.896
LM	42.305	34.429	−25.182	109.791
GAM smooth	46.635	40.358	−32.475	125.745
GAM tensor	49.009	32.855	−15.394	113.412
KNN	82.516	30.388	22.949	142.083

Note: Shown are estimates of $\theta_{i,j}$ (in degrees) and $h_{i,j}$ (in milligrams) for the nutritional trade-off between life span and reproductive rate. Analysis is from the data presented in Lee et al. (2008). Confidence intervals overlapping zero implies no difference in the peaks. Magnitude of the estimates indicate the strength of nutritional trade-offs (i.e., larger magnitudes indicate stronger nutritional trade-offs). Note that $\theta_{i,j}$ is bound between 0 and 90 degrees (i.e., 0 and $\pi/2$). Bayes = Bayesian linear regression; GAM = generalized additive model; GBoost = gradient boost; KNN = k-nearest neighbors; LM = general linear regression; RF = random forest; SVM = support-vector machine.

describe nutritional trade-offs in multidimensional performance landscapes for data of different structures.

Comparing Trait Optimum with Intake Target

When given a choice of imbalanced diets, animals balance their nutrient intake to ratios that maximize the expression of some fitness traits at the expense of others. In the landmark data set used here, *Drosophila melanogaster* flies balanced their P:C to a ratio of 1:4, which does not coincide with the P:C ratios that maximize life span or reproductive rate (Lee et al. 2008). We tested whether nutrigonometry could identify such known nutritional trade-off in the data. All models predicted a significantly

Table 2: Estimates of nutritional compromises

Data, trait, model	Mean	Confidence interval		Target (visual)
		Upper	Lower	
Peak ratio (intakes):				
Life span				16
GBoost	5.235	5.205	5.265	
RF	5.533	5.508	5.557	
SVM	5.864	5.836	5.892	
LM	9.084	9.048	9.120	
Bayes	9.154	9.118	9.190	
KNN	12.075	12.015	12.135	
GAM smooth	13.055	12.997	13.114	
GAM tensor	13.108	13.049	13.168	
Reproductive rate				2
GBoost	1.858	1.853	1.864	
KNN	2.041	2.037	2.045	
RF	2.138	2.133	2.144	
SVM	2.147	2.138	2.156	
Bayes	2.194	2.191	2.197	
LM	2.215	2.212	2.219	
GAM smooth	2.644	2.639	2.650	
GAM tensor	2.661	2.656	2.667	
Peak ratio (fixed):				
Life span				16
GBoost	13.078	12.987	13.170	
SVM	14.946	14.873	15.019	
RF	15.107	15.045	15.169	
GAM smooth	16.977	16.859	17.097	
GAM tensor	20.623	20.536	20.710	
KNN	26.050	25.929	26.173	
Bayes	32.426	32.237	32.617	
LM	32.933	32.744	33.125	
Reproductive rate				2
KNN	1.467	1.463	1.470	
LM	1.836	1.832	1.839	
Bayes	1.841	1.837	1.845	
GBoost	2.171	2.168	2.174	
GAM tensor	2.244	2.241	2.248	
RF	2.545	2.539	2.552	
SVM	3.527	3.516	3.538	
GAM smooth	4.280	4.265	4.296	

Note: Shown are estimates of optimal intake that maximizes life span and reproductive rate based on the predicted peak region. Comparison is made with the visual peak ratio from Lee et al. (2008). Note that all but one model (i.e., generalized additive model [GAM] smooth for fixed ratio reproductive rate data) predicted a peak region of ~1:4, which is the ratio that individuals balance when given the ability to balance their diet. Other models suggest that a P:C ratio of 1:4 is lower than the ratio needed to maximize life span but higher than that for reproductive rate. Bayes = Bayesian linear regression; GBoost = gradient boost; KNN = *k*-nearest neighbors; LM = general linear regression; RF = random forest; SVM = support-vector machine.

lower optimum P:C ratio that maximizes reproductive rate relative to life span, as expected from the original visual comparison of landscapes (around 1:2 for reproductive rate and >1:9 for life span; table 2). However, none of the estimates overlapped the P:C ratio of 1:4. This confirms the findings from the original study that *D. melanogaster* females do not balance their nutrient intake to maximize life span or reproductive rate but instead balance their P:C to 1:4 in order to maximize lifetime egg production (Lee et al. 2008). This validates the power of nutrigonometry in analyzing nutritional behavior in GF studies (Lee et al. 2008).

Discussion

We introduced a new simple analytical framework to analyze nutritional trade-offs in multidimensional fitness landscapes. Nutrigonometry uses trigonometric relationships from right-angle triangles to identify and compare peaks (or valleys) in 3D performance landscapes. Using a landmark GF data set, we demonstrated the precision and performance of standard statistical (machine learning) models in finding the peak regions in performance landscapes and subsequently quantifying the strength of nutritional trade-offs between traits. In the first comparative analysis of statistical methods in GF data sets, we showed that simpler general linear models outshined machine learning models in the prediction of peak and valley regions in the performance landscapes. Thus, nutrigonometry is a powerful yet easy-to-implement methodology to determine the strength of nutritional trade-offs in fitness studies in the field of animal nutrition.

Multidimensional studies of nutrition through the GF have been increasingly used to gain insight into animal and human nutrition (Lee et al. 2008; Behmer 2009; Felton et al. 2009; Simpson and Raubenheimer 2012; Hewson-Hughes et al. 2013; Gosby et al. 2014; Solon-Biet et al. 2014). Likewise, the complexity of the applications has also increased, ranging from studies with few nutrients (e.g., protein and carbohydrates, salts) through to high-dimensional studies investigating individual fatty acids and amino acids (Simpson et al. 2006; Grandison et al. 2009; Arien et al. 2015; Arganda et al. 2017; Piper et al. 2017). This means that analytical frameworks that are simple and robust must be developed to support the development of the field.

In this study, we introduced such a framework. Previous methods were either computationally expensive (and imprecise) or could, in some cases, overestimate the strength of nutritional trade-offs. For instance, Rapkin et al. (2018) proposed a model that used regression slopes of the nutrients onto the performance trait as coordinates of a vector v_i for performance trait i. From these vectors, the angle θ' between vectors v_i and v_j for traits i and j, respectively, could be calculated as the estimate of the strength of the nutritional trade-off. This method has the limitation that regression slopes can be positive, zero, or negative, whereas performance landscapes can exist only in the positive numbers (i.e., animals cannot eat negative amounts of nutrients). This can lead to overestimation of nutritional trade-offs (Morimoto and Lihoreau 2019). We then proposed a method, known as the vector of positions approach, that addressed this limitation and used vectors with coordinates that matched the location of peaks in the domain of positive numbers (Morimoto and Lihoreau 2019). However, this approach was limited because (i) we used an SVM model that required an arbitrary input threshold to identify peaks and (ii) was computationally expensive to apply to multiple landscapes. Nutrigonometry resolves the limitations from the previous models as it (1) estimates nutritional trade-offs using the domain of positive numbers; (2) demonstrates, in the first comparative study of statistical methods, that simpler (Bayesian) linear regressions are often more precise; and (3) is computationally cheap to run, as it relies on simple trigonometric relationships. Thus, nutrigonometry enables reliable large-scale studies of the fitness consequences of animal foraging decisions that will shed light onto the evolution of physiological and behavioral responses to nutrition.

We have provided the first comparative assessment of the power and precision of common statistical models in identifying regions of interest (e.g., peaks or valleys) in multidimensional performance landscapes. More importantly, we have shown that nutrigonometry provides a clear, concise, and simpler foundation to analyzing GF data by demonstrating the best approach to investigate nutritional trade-offs in 3D fitness landscapes. Because nutrigonometry uses trigonometric relationships of right-angle triangles, it is applicable to n dimensions. However, given the often counterintuitive geometrical effects of high dimensionality (e.g., Milman 1998; Watanabe 2021), such expansion to higher dimensions requires further investigation as the topic of future developments. Nevertheless, given the broad use of 3D fitness landscapes in GF studies (Morimoto and Lihoreau 2020), nutrigonometry readily enables important quantifications of nutritional trade-offs that were otherwise absent or cumbersome to produce. For instance, using a range of models, nutrigonometry uses right-angle triangles to compare the ratio of nutrients that maximize life span and reproductive rate along with the strength of nutritional trade-offs between these traits in a landmark article in the field (Lee et al. 2008). Moreover, nutrigonometry is capable of comparing the nutrient ratio that maximizes life span and reproductive rate with the nutrient ratio that is balanced by individuals when given a choice, providing important insights into the dietary choices underpinning nutritional compromises. Such quantification can bring new fundamental insights into our understanding of nutritional trade-offs, such as the strength and direction of the trade-offs (e.g., nutrient balance vs. concentration; see fig. 1), as well as how much animals actually resolve these trade-offs when they have the opportunity to do so and whether, for instance, they favor one trait over another (distance between optimal trade-off and observed nutrient intake target; see table 2).

An important trend in the field of multidimensional nutrition is the study of nutritional effects across physiological pathways and across levels of biological organization (Lihoreau et al. 2014; Simpson et al. 2015). These studies generate multiple performance landscapes that

are often compared visually, without rigorous analytical methods to measure nutritional trade-offs. This limits our ability to identify diet balances that maximize (or minimize) the gene expression of a particular pathway. For example, regions of 11 performance landscapes of the expression of genes involved in the insulin/insulin-like growth factor (IGF) pathway were visually compared to provide insights into how a key endocrine pathway is regulated on the basis of nutrient intake and how gene expression can underlie expression of life histories (Post and Tatar 2016; McDonald et al. 2021). Likewise, regions of 12 performance landscapes with gut microbial diversity or abundance were visually compared to better understand how nutrient composition can modulate host-microbe interactions (Ng et al. 2019). Similar visual comparisons have been made to understand the effects of nutrition on host-endosymbiont relationships (Ponton et al. 2015). Of course, the goal of these molecular studies may not have been the identification of nutrient ratios that optimize (or minimize) gene expression but instead the relative contribution of specific nutrients to changes in the gene expression profile. Nevertheless, identifying peaks and valleys in GF gene expression landscapes is a useful concept with wider application to veterinary and medical sciences (Simpson and Raubenheimer 2009). Nutrigonometry will allow researchers to move beyond visual comparisons to quantitatively assess how landscapes differ using a rigorous and reproducible framework, providing (additional) tools for better understanding the properties of multidimensional performance landscapes. As a result, nutrigonometry yields considerable advances to the status quo in the field, enabling a deeper understanding of the role of nutrition in physiology, behavior, and ecology.

Conclusion

We propose a model that is simple and robust to analyze performance landscapes from GF studies. Contrary to previous methods (Rapkin et al. 2018; Morimoto and Lihoreau 2019), nutrigonometry does not rely on vector calculations but instead harnesses the trigonometric relationships of right-angle triangles to estimate nutritional trade-offs. This is a major advance of the model, as it considerably simplifies the framework in both conceptual and computational terms. Nutrigonometry thus significantly advances our ability to generate reliable and reproducible estimates of nutritional trade-offs within and between species, facilitating quantitative studies of animal nutrition within and between species. These advances in our approach opens new avenues of research in multidimensional nutrition and allows for physiological and comparative studies to be performed in a consistent and reproducible way from which insights into the evolution of animal nutrition can be gained across the tree of life.

Acknowledgments

J.M. is supported by the Biotechnology and Biological Sciences Research Council (BBSRC; BB/V015249/1). P.C. is supported by the Engineering and Physical Sciences Research Council (EPSRC; EP/P025072/) and the École Polytechnique Fédérale de Lausanne via a collaboration agreement with the University of Aberdeen. M.L. receives support from the Centre national de la recherche scientifique (CNRS), the French Research Agency (ANR 3DNaviBee: ANR-19-CE37-0024), the French Environment and Energy Management Agency (ADEME LOTAPIS), the European Regional Development Fund (FEDER ECONECT: MP0021763), and the European Research Council (ERC-CoG BEE-MOVE: GA101002644). We thank Kwang Lee, Teresa Kutz, and Carla Sgrò for kindly sharing the data that was used to demonstrate the use of our model. We thank Gordon M. Hay for the translation of our abstract into Doric.

Statement of Authorship

Conceptualization: J.M.; methods development/experimental design: J.M.; data collection: J.M.; data analysis: J.M., P.C., C.M., M.L.; data validation: J.M.; data visualization: J.M.; model analysis: J.M. with input from P.C., C.M., M.L.; coding simulation: J.M.; writing—original draft: J.M., P.C.; writing—review and editing: J.M., C.M., M.L. All authors approved the submission of the final version of the manuscript.

Data and Code Availability

Kutz et al. (2019) data are available at https://doi.org/10.26180/5cfe1ddaaafac. The Lee et al. data set (2008) is available in Dryad (https://doi.org/10.5061/dryad.tp7519s). R scripts with functions for the implementation of the nutrigonometry framework are available in Dryad Digital Repository and Zenodo (Morimoto et al. 2022; https://doi.org/10.5061/dryad.5mkkwh78q).

Literature Cited

Arganda, S., S. Bouchebti, S. Bazazi, S. Le Hesran, C. Puga, G. Latil, S. J. Simpson, et al. 2017. Parsing the life-shortening effects of dietary protein: effects of individual amino acids. Proceedings of the Royal Society B 284:20162052.

Arien, Y., A. Dag, S. Zarchin, T. Masci, and S. Shafir. 2015. Omega-3 deficiency impairs honey bee learning. Proceedings of the National Academy of Sciences of the USA 112:15761–15766.

Barragan-Fonseca, K. B., M. Dicke, and J. J. A. van Loon. 2018. Influence of larval density and dietary nutrient concentration on performance, body protein, and fat contents of black soldier fly larvae (*Hermetia illucens*). Entomologia Experimentalis et Applicata 166:761–770.

Barragan-Fonseca, K. B., G. Gort, M. Dicke, and J. J. A. van Loon. 2021. Nutritional plasticity of the black soldier fly (*Hermetia illucens*) in response to artificial diets varying in protein and carbohydrate concentrations. Journal of Insects as Food and Feed 7:51–61.

Behmer, S. T. 2009. Insect herbivore nutrient regulation. Annual Review of Entomology 54:165–187.

Bunning, H., J. Rapkin, L. Belcher, C. R. Archer, K. Jensen, and J. Hunt. 2015. Protein and carbohydrate intake influence sperm number and fertility in male cockroaches, but not sperm viability. Proceedings of the Royal Society B 282:20142144.

Fanson, B., and P. W. Taylor. 2012. Protein : carbohydrate ratios explain life span patterns found in Queensland fruit fly on diets varying in yeast : sugar ratios. Age (Dordr) 34:1361–1368.

Fanson, B., S. Yap, and P. W. Taylor. 2012. Geometry of compensatory feeding and water consumption in *Drosophila melanogaster*. Journal of Experimental Biology 215:766–773.

Felton, A. M., A. Felton, D. Raubenheimer, S. J. Simpson, W. J. Foley, J. T. Wood, I. R. Wallis, et al. 2009. Protein content of diets dictates the daily energy intake of a free-ranging primate. Behavioral Ecology 20:685–690.

Gage, M. J. G., and P. A. Cook. 1994. Sperm size or numbers—effects of nutritional stress upon eupyrene and apyrene sperm production strategies in the moth *Plodia interpunctella* (Lepidoptera: Pyralidae). Functional Ecology 8:594–599.

Goodrich, B., J. Gabry, I. Ali, and S. Brilleman. 2020. rstanarm: Bayesian applied regression modeling via Stan. R package, version 2.19.2.

Gosby, A. K., A. D. Conigrave, D. Raubenheimer, and S. J. Simpson. 2014. Protein leverage and energy intake. Obesity Reviews 15:183–191.

Grandison, R. C., M. D. W. Piper, and L. Partridge. 2009. Amino-acid imbalance explains extension of lifespan by dietary restriction in *Drosophila*. Nature 462:1061–1064.

Guo, J.-W., Y. Cui, P.-J. Lin, B.-P. Zhai, Z.-X. Lu, J. W. Chapman, and G. Hu. 2022. Male nutritional status does not impact the reproductive potential of female *Cnaphalocrocis medinalis* moths under conditions of nutrient shortage. Insect Science 29:467–477.

Harrison, S. J., D. Raubenheimer, S. J. Simpson, J.-G. J. Godin, and S. M. Bertram. 2014. Towards a synthesis of frameworks in nutritional ecology: interacting effects of protein, carbohydrate and phosphorus on field cricket fitness. Proceedings of the Royal Society B 281:20140539.

Hewson-Hughes, A. K., V. L. Hewson-Hughes, A. Colyer, A. T. Miller, S. J. McGrane, S. R. Hall, R. F. Butterwick, et al. 2013. Geometric analysis of macronutrient selection in breeds of the domestic dog, *Canis lupus familiaris*. Behavioral Ecology 24:293–304.

Hewson-Hughes, A. K., V. L. Hewson-Hughes, A. T. Miller, S. R. Hall, S. J. Simpson, and D. Raubenheimer. 2011. Geometric analysis of macronutrient selection in the adult domestic cat, *Felis catus*. Journal of Experimental Biology 214:1039–1041.

Hope, R. M. 2013. Package "Rmisc." https://CRAN.R-project.org/package = Rmisc.

Hunt, J., R. Brooks, M. D. Jennions, M. J. Smith, C. L. Bentsen, and L. F. Bussiere. 2004. High-quality male field crickets invest heavily in sexual display but die young. Nature 432:1024–1027.

Jensen, K., C. McClure, N. K. Priest, and J. Hunt. 2015. Sex-specific effects of protein and carbohydrate intake on reproduction but not lifespan in *Drosophila melanogaster*. Aging Cell 14:605–615.

Kutz, T. C., C. M. Sgrò, and C. K. Mirth. 2019. Interacting with change: diet mediates how larvae respond to their thermal environment. Functional Ecology 33:1940–1951.

Lee, K. P., S. J. Simpson, F. J. Clissold, R. Brooks, J. W. Ballard, P. W. Taylor, N. Soran, et al. 2008. Lifespan and reproduction in *Drosophila*: new insights from nutritional geometry. Proceedings of the National Academy of Sciences of the USA 105:2498–2503.

Lihoreau, M., J. Buhl, M. A. Charleston, G. A. Sword, D. Raubenheimer, and S. J. Simpson. 2014. Modelling nutrition across organizational levels: from individuals to superorganisms. Journal of Insect Physiology 69:2–11.

Ma, C., C. K. Mirth, M. D. Hall, and M. D. W. Piper. 2020. Amino acid quality modifies the quantitative availability of protein for reproduction in *Drosophila melanogaster*. Journal of Insect Physiology 139:104050.

Maklakov, A. A., S. J. Simpson, F. Zajitschek, M. D. Hall, J. Dessmann, F. Clissold, D. Raubenheimer, et al. 2008. Sex-specific fitness effects of nutrient intake on reproduction and lifespan. Current Biology 18:1062–1066.

McDonald, J. M. C., P. Nabili, L. Thorsen, S. Jeon, and A. W. Shingleton. 2021. Sex-specific plasticity and the nutritional geometry of insulin-signaling gene expression in *Drosophila melanogaster*. EvoDevo 12:1–17.

Milman, V. 1998. Surprising geometric phenomena in high-dimensional convexity theory. Pages 73–91 *in* European Congress of Mathematics. Springer, London.

Morimoto, J., P. Conceição, C. Mirth, and M. Lihoreau. 2022. Data from: Nutrigonometry I: using right-angle triangles to quantify nutritional trade-offs in performance landscapes. American Naturalist, Dryad Digital Repository, https://doi.org/10.5061/dryad.5mkkwh78q.

Morimoto, J., and M. Lihoreau. 2019. Quantifying nutritional trade-offs across multidimensional performance landscapes. American Naturalist 193:E168–E181.

———. 2020. Open data for open questions in comparative nutrition. Insects 11:236.

Morimoto, J., A. Senior, K. Ruiz, J. A. Wali, T. Pulpitel, S. M. Solon-Biet, V. C. Cogger, et al. 2019. Sucrose and starch intake contribute to reduced alveolar bone height in a rodent model of naturally occurring periodontitis. PLoS ONE 14:e0212796.

Morimoto, J., and S. Wigby. 2016. Differential effects of male nutrient balance on pre-and post-copulatory traits, and consequences for female reproduction in *Drosophila melanogaster*. Scientific Reports 6:1–12.

Ng, S. H., S. J. Simpson, and L. W. Simmons. 2018. Macronutrients and micronutrients drive trade-offs between male pre- and post-mating sexual traits. Functional Ecology 32:2380–2394.

Ng, S. H., M. Stat, M. Bunce, S. J. Simpson, and L. W. Simmons. 2019. Protein and carbohydrate intakes alter gut microbial community structure in crickets: a Geometric Framework approach. FEMS Microbiology Ecology 95:fiz106.

Nychka, D., F. Reinhard, J. Paige, and S. Sain. 2017. fields: tools for spatial data. R package, version 9.9.

Piper, M. D. W., G. A. Soultoukis, E. Blanc, A. Mesaros, S. L. Herbert, P. Juricic, X. He, et al. 2017. Matching dietary amino acid balance to the in silico-translated exome optimizes growth and reproduction without cost to lifespan. Cell Metabolism 25:610–621.

Polak, M., L. W. Simmons, J. B. Benoit, K. Ruohonen, S. J. Simpson, and S. M. Solon-Biet. 2017. Nutritional geometry of paternal effects on embryo mortality. Proceedings of the Royal Society B 284:20171492.

Ponton, F., J. Morimoto, K. Robinson, S. S. Kumar, S. C. Cotter, K. Wilson, and S. J. Simpson. 2019. Macronutrients modulate survival to infection and immunity in *Drosophila*. Journal of Animal Ecology 89:460–470.

Ponton, F., K. Wilson, S. C. Cotter, D. Raubenheimer, and S. J. Simpson. 2011. Nutritional immunology: a multi-dimensional approach. PLoS Pathogens 7:e1002223.

Ponton, F., K. Wilson, A. Holmes, D. Raubenheimer, K. L. Robinson, and S. J. Simpson. 2015. Macronutrients mediate the functional relationship between *Drosophila* and *Wolbachia*. Proceedings of the Royal Society B 282:20142029.

Post, S., and M. Tatar. 2016. Nutritional geometric profiles of insulin/IGF expression in *Drosophila melanogaster*. PLoS ONE 11: e0155628.

Rapkin, J., K. Jensen, C. R. Archer, C. M. House, S. K. Sakaluk, E. Del Castillo, and J. Hunt. 2018. The geometry of nutrient space-based life-history trade-offs: sex-specific effects of macronutrient intake on the trade-off between encapsulation ability and reproductive effort in decorated crickets. American Naturalist 191:452–474.

Raubenheimer, D., and S. J. Simpson. 1993. The geometry of compensatory feeding in the locust. Animal Behaviour 45:953–964.

———. 2020. Eat like the animals: what nature teaches us about the science of healthy eating. Houghton Mifflin, New York.

R Core Team. 2019. R: a language and environment for statistical computing. R Foundation for Statistical Computing, Vienna.

Roff, D. A. 2002. Life history evolution. Sinauer, Princeton, NJ.

Schwenke, R. A., B. P. Lazzaro, and M. F. Wolfner. 2016. Reproduction–immunity trade-offs in insects. Annual Review of Entomology 61:239–256.

Simpson, S. J., F. J. Clissold, M. Lihoreau, F. Ponton, S. M. Wilder, and D. Raubenheimer. 2015. Recent advances in the integrative nutrition of arthropods. Annual Review of Entomology 60:293–311.

Simpson, S. J., D. G. Le Couteur, D. E. James, J. George, J. E. Gunton, S. M. Solon-Biet, and D. Raubenheimer. 2017. The Geometric Framework for Nutrition as a tool in precision medicine. Nutrition and Healthy Aging 4:217–226.

Simpson, S. J., and D. Raubenheimer. 1993. A multi-level analysis of feeding behaviour: the geometry of nutritional decisions. Philosophical Transactions of the Royal Society B 342:381–402.

———. 2009. Macronutrient balance and lifespan. Aging 1:875.

———. 2012. The nature of nutrition: a unifying framework from animal adaptation to human obesity. Princeton University Press, Princeton, NJ.

Simpson, S. J., G. A. Sword, P. D. Lorch, and I. D. Couzin. 2006. Cannibal crickets on a forced march for protein and salt. Proceedings of the National Academy of Sciences of the USA 103:4152–4156.

Solon-Biet, S. M., A. C. McMahon, J. W. O. Ballard, K. Ruohonen, L. E. Wu, V. C. Cogger, A. Warren, et al. 2014. The ratio of macronutrients, not caloric intake, dictates cardiometabolic health, aging, and longevity in ad libitum-fed mice. Cell Metabolism 19:418–430.

Stearns, S. C. 1992. The evolution of life histories. Oxford University Press, Oxford.

Treidel, L. A., R. M. Clark, M. T. Lopez, and C. M. Williams. 2021. Physiological demands and nutrient intake modulate a trade-off between dispersal and reproduction based on age and sex of field crickets. Journal of Experimental Biology 224:jeb237834.

Wadhwa, R. R., D. F. K. Williamson, A. Dhawan, and J. G. Scott. 2018. TDAstats: R pipeline for computing persistent homology in topological data analysis. Journal of Open Source Software 3:860.

Watanabe, J. 2021. Detecting (non)parallel evolution in multidimensional spaces: angles, correlations, and eigenanalysis. EcoEvoRxiv, https://doi.org/10.32942/osf.io/2gxwb.

Weinberger, S. 2011. What is . . . persistent homology? Notices of the AMS 58:36–39.

Wickham, H. 2016. ggplot2: elegant graphics for data analysis. Springer, Berlin.

Wickham, H., M. Averick, J. Bryan, W. Chang, L. D. McGowan, R. François, G. Grolemund, et al. 2019. Welcome to the Tidyverse. Journal of Open Source Software 4:1686.

Wood, S., and M. S. Wood. 2015. Package "mgcv." R package, version 1.29.

Zomorodian, A., and G. Carlsson. 2005. Computing persistent homology. Discrete and Computational Geometry 33:249–274.

References Cited Only in the Online Enhancements

Adams, H., and M. Moy. 2021. Topology applied to machine learning: from global to local. Frontiers in Artificial Intelligence 4:54.

Chazal, F., and B. Michel. 2021. An introduction to topological data analysis: fundamental and practical aspects for data scientists. Frontiers in Artificial Intelligence 4:1–21.

Conceição, P., and J. Morimoto. 2022. "Holey" niche! finding holes in niche hypervolumes using persistence homology. *Journal of Mathematical Biology* 84:58.

Ghrist, R. 2008. Barcodes: the persistent topology of data. Bulletin of the American Mathematical Society 45:61–75.

———. 2014. Elementary applied topology. Createspace, Seattle, WA.

Gray, L. J., S. J. Simpson, and M. Polak. 2018. Fruit flies may face a nutrient-dependent life-history trade-off between secondary sexual trait quality, survival and developmental rate. Journal of Insect Physiology 104:60–70.

Hatcher, A. 2002. Algebraic topology. Cambridge University Press, Cambridge.

Jang, T., and K. P. Lee. 2018. Comparing the impacts of macronutrients on life-history traits in larval and adult *Drosophila melanogaster*: the use of nutritional geometry and chemically defined diets. Journal of Experimental Biology 221:jeb181115. https://doi.org/10.1242/jeb.181115.

Otter, N., M. A. Porter, U. Tillmann, P. Grindrod, and H. A. Harrington. 2017. A roadmap for the computation of persistent homology. EPJ Data Science 6:1–38.

Rodrigues, M. A., N. E. Martins, L. F. Balancé, L. N. Broom, A. J. S. Dias, A. S. D. Fernandes, and C. K. Mirth. 2015. *Drosophila melanogaster* larvae make nutritional choices that minimize developmental time. Journal of Insect Physiology 81:69–80. https://doi.org/10.1016/j.jinsphys.2015.07.002.

Runagall-McNaull, A., R. Bonduriansky, and A. J. Crean. 2015. Dietary protein and lifespan across the metamorphic boundary: protein-restricted larvae develop into short-lived adults. Scientific Reports 5:11783. https://doi.org/10.1038/srep11783.

Associate Editor: Lisa E. Schwanz
Editor: Erol Akçay